respectively. In media with glucose (*GAL1* promoter inactive), both soluble and bound boron concentrations were similar between yeast lines (data not shown).

Analysis of boron concentration

Determination of boron concentration by inductively coupled plasma mass spectrometry were performed as described previously[7,8,11] with some modifications (see Supplementary Information 6). Tracer boron concentrations were calculated as described previously[7].

Received 28 January; accepted 3 September 2002; doi:10.1038/nature01139.

1. Shorrocks, V. M. The occurrence and correction of boron deficiency. *Plant Soil* **193,** 121–148 (1997).
2. Dannel, F., Pfeffer, H. & Römheld, V. Update on boron in higher plants – uptake, primary translocation and compartmentation. *Plant Biol.* **4,** 193–204 (2002).
3. Brown, P. H. *et al.* Boron in plant biology. *Plant Biol.* **4,** 205–223 (2002).
4. O'Neill, M. A., Eberhard, S., Albersheim, P. & Darvill, A. G. Requirement of borate cross-linking of cell wall rhamnogalacturonan II for *Arabidopsis* growth. *Science* **294,** 846–849 (2001).
5. Nielsen, F. H. The emergence of boron as nutritionally important throughout the life cycle. *Nutrition* **16,** 512–514 (2000).
6. Bennett, A., Rowe, R. I., Soch, N. & Eckhert, C. D. Boron stimulates yeast (*Saccharomyces cerevisiae*) growth. *J. Nutr.* **129,** 2236–2238 (1999).
7. Noguchi, K. *et al. bor1-1*, an *Arabidopsis thaliana* mutant that requires a high level of boron. *Plant Physiol.* **115,** 901–906 (1997).
8. Takano, J., Yamagami, M., Noguchi, K., Hayashi, H. & Fujiwara, T. Preferential translocation of boron to young leaves in *Arabidopsis thaliana* regulated by the *BOR1* gene. *Soil Sci. Plant Nutr.* **47,** 345–357 (2001).
9. Dannel, F., Pfeffer, H. & Römheld, V. Characterization of root boron pools, boron uptake and boron translocation in sunflower using the stable isotopes ^{10}B and ^{11}B. *Aust. J. Plant Physiol.* **27,** 397–405 (2000).
10. Stangoulis, J. C. R., Reid, R. J., Brown, P. H. & Graham, R. D. Kinetic analysis of boron transport in *Chara*. *Planta* **213,** 142–146 (2001).
11. Noguchi, K. *et al.* Defect in root-shoot translocation of boron in *Arabidopsis thaliana* mutant *bor1-1*. *J. Plant Physiol.* **156,** 751–755 (2000).
12. Poirier, Y., Thoma, S., Somerville, C. & Schiefelbein, J. A mutant of *Arabidopsis* deficient in xylem loading of phosphate. *Plant Physiol.* **97,** 1087–1093 (1991).
13. Gaymard, F. *et al.* Identification and disruption of a plant shaker-like outward channel involved in K^+ release into the xylem sap. *Cell* **94,** 647–655 (1998).
14. Dannel, F., Pfeffer, H. & Römheld, V. Compartmentation of boron in roots and leaves of sunflower as affected by boron supply. *J. Plant Physiol.* **153,** 615–622 (1998).
15. Yasumori, M., *et al. Plant Nutrition: Molecular Biology and Genetics* (eds Nielsen, G. G. & Jensen, A.) 269–275 (Kluwer, Dordrecht, 1999).
16. Alper, S. L., Darman, R. B., Chernova, M. N. & Dahl, N. K. The AE gene family of Cl^-/HCO_3^- exchangers. *J. Nephrol.* **15** suppl. 5, S41–S53 (2002).
17. Soleimani, M. Na^+:HCO_3^- cotransporters (NBC): Expression and regulation in the kidney. *J. Nephrol.* **15 suppl. 5,** S32–S40 (2002).
18. Pearson, W. R. & Lipman, D. J. Improved tools for biological sequence comparison. *Proc. Natl Acad. Sci. USA* **85,** 2444–2448 (1988).
19. Zhao, R. & Reithmeier, R. A. F. Expression and characterization of the anion transporter homologue YNL275w in *Saccharomyces cerevisiae*. *Am. J. Physiol. Cell Physiol.* **281,** C33–C45 (2001).
20. Chiu, W. L. *et al.* Engineered GFP as a vital reporter in plants. *Curr. Biol.* **6,** 325–330 (1996).
21. Raven, J. A. Short- and long-distance transport of boric acid in plants. *New Phytol.* **84,** 231–249 (1980).
22. Dordas, C., Chrispeels, M. J. & Brown, P. H. Permeability and channel-mediated transport of boric acid across membrane vesicles isolated from squash roots. *Plant Physiol.* **124,** 1349–1361 (2000).
23. Dordas, C. & Brown, P. H. Permeability and the mechanism of transport of boric acid across the plasma membrane of *Xenopus laevis* oocytes. *Biol. Trace Elem. Res.* **81,** 127–139 (2001).
24. Jefferson, R. A., Kavanagh, T. A. & Bevan, M. W. GUS fusions: beta-glucuronidase as a sensitive and versatile gene fusion marker in higher plants. *EMBO J.* **6,** 3901–3907 (1987).
25. Deblaere, R. *et al.* Efficient octopine Ti plasmid-derived vectors for Agrobacterium-mediated gene transfer to plants. *Nucleic Acids Res.* **13,** 4777–4788 (1985).
26. Bechtold, N., Ellis, J. & Pelletier, G. *In planta* Agrobacterium mediated gene transfer by infiltration of adult *Arabidopsis thaliana* plants. *C.R. Acad. Sci. Paris Life Sci.* **316,** 1194–1199 (1993).
27. Fujiwara, T., Hirai, M. Y., Chino, M., Komeda, Y. & Naito, S. Effects of sulfur nutrition on expression of the soybean seed storage protein genes in transgenic petunia. *Plant Physiol.* **99,** 263–268 (1992).
28. Winzeler, E. A. *et al.* Functional characterization of the *S. cerevisiae* genome by gene deletion and parallel analysis. *Science* **285,** 901–906 (1999).
29. Sherman, F. Getting started with yeast. *Method. Enzymol.* **194,** 3–21 (1991).
30. Kyte, J. & Doolittle, R. F. A simple method for displaying the hydropathic character of a protein. *J. Mol. Biol.* **157,** 105–132 (1982).

Supplementary Information accompanies the paper on *Nature*'s website (http://www.nature.com/nature).

Acknowledgements We thank S. Naito, N. von Wirén and P. Walch-Liu for critical reading of the manuscript; Y. Niwa for providing the sGFP construct; K. Mukaikawato, M. Hashimoto and M. Sugasawa for technical contributions; and F. Kurisu for use of the facilities of the Research Center for Water Environment Technology in the School of Engineering, the University of Tokyo. RZ119b07 was kindly provided by Kazusa DNA Research Institute; BAC T3D7 clone was kindly provided by the *Arabidopsis* Biological Resource Center at Ohio State University. This work is supported in part by grants to T.F. from the Japanese Ministry of Education, Sports, Culture, Science, and Technology and the Graduate School of Agricultural Life Sciences, the University of Tokyo.

Competing interests statement The authors declare competing financial interests: details accompany the paper on *Nature*'s website (http://www.nature.com).

Correspondence and requests for materials should be addressed to T.F. (e-mail: atorufu@mail.ecc.u-tokyo.ac.jp) Genbank accession number of BOR1 is AB073713.

In silico simulations reveal that replicators with limited dispersal evolve towards higher efficiency and fidelity

Péter Szabó*†, István Scheuring*, Tamás Czárán* & Eörs Szathmáry*‡

** Department of Plant Taxonomy and Ecology, Research Group of Ecology and Theoretical Biology, Eötvös University, 1/c Pázmány P. sétány, H-1117 Budapest*
† Adaptive Dynamics Network, International Institute for Applied Systems Analysis, A-2361 Laxenburg, Austria
‡ Collegium Budapest (Institute for Advanced Study) 2 Szentháromság u., H-1014 Budapest, Hungary

The emergence of functional replicases, acting quickly and with high accuracy, was crucial to the origin of life[1]. Although where the first RNA molecules came from is still unknown, it is nevertheless assumed that catalytic RNA enzymes (ribozymes) with replicase function emerged at some early stage of evolution[1]. The fidelity of copying is especially important because the mutation load limits the length of replicating templates that can be maintained by natural selection[2]. An increase in template length is disadvantageous for a fixed digit copying fidelity, however, longer molecules are expected to be better replicases. An iteration for longer molecules with better replicase function has been suggested[3,4] and analysed mathematically[5]. Here we show that more efficient replicases can spread, provided they are adsorbed to a prebiotic mineral surface. A cellular automaton[6] simulation reveals that copying fidelity, replicase speed and template efficiency all increase with evolution, despite the presence of molecular parasites, essentially because of reciprocal atruism[7] ('within-species mutualism') on the surface[8], thus making a gradual improvement of replicase function more plausible.

We considered a population of macromolecules, adsorbed to a surface and built of four different monomers: A, B, C and D. Owing to their catalytic activity, macromolecules located on neighbouring sites of the surface can template-replicate each other, that is, they can build a new macromolecule from free monomers by copying an existing one. In each replication process there are two replicator molecules involved: one is the template, the other acts as a replicase enzyme. We attributed two main properties to replication events: speed and fidelity, which in turn depend on three parameters of the two replicators involved in the process: (1) replicase activity, which expresses how fast the molecule can add a monomer to a new strain while acting as a replicase; (2) replicase fidelity, which measures the accuracy of replication per monomer when the molecule acts as a replicase; (3) template efficiency, which defines the average 'affinity' of the molecule, that is, its tendency to behave as a template against others.

Replication speed depends on the activity of the replicase and the quality of the template (as explained below in detail) such that higher replicase activity and template efficiency result in faster replication. Given two neighbouring replicator molecules, L and M, on the surface, one of two different replication events can occur: either L as a replicase copies M as a template, or vice versa.

For simplicity, we assumed that replicase activity, replicase fidelity and template efficiency depend on the primary structure of the replicator molecule as follows: A, B and C type monomers each affect one of the three relevant replicator properties: A enhances template efficiency, B increases replicase activity, and C is beneficial in terms of replicase fidelity. D is a neutral ('dummy') monomer of no direct effect on replication. We assumed that the template efficiency $t(n_A)$ of a certain replicator molecule is an

increasing sigmoid function of the number n_A of A monomers in the longest contiguous poly-A section within the macromolecule:

$$t(n_A) = \alpha_A + (1 - \alpha_A)\frac{n_A^{\beta_A}}{\gamma_A + n_A^{\beta_A}} \quad \text{if} \quad n_A > 0 \tag{1}$$

$$t(n_A) = 0 \quad \text{if} \quad n_A = 0 \tag{2}$$

With appropriate $\alpha_B, \beta_B, \gamma_B$ and $\alpha_C, \beta_C, \gamma_C$ parameters, replicase activity $r(n_B)$ and replicase fidelity $f(n_C)$ were defined as increasing sigmoid functions of the lengths of contiguous poly-B and poly-C sections in the macromolecule, applying the same mathematical form. Minimal fidelity (at 0 poly-C sequence length) was set to values of 0.7 to 0.9 in different simulations (random monomer insertion itself implies a fidelity of 0.25). Our rationale for choosing a sigmoid function is as follows: (1) There should be saturation after a sufficient number of monomers involved (equivalent to diminishing returns). One reason for this is that the reactions become diffusion-limited, especially on a surface. (2) If a number of critical sites are involved in forming a working active centre, then it is reasonable to assume that there is a synergistic effect between these sites when the molecules are small. The combination of these two effects results in a sigmoid function.

Our modelling of domains that are responsible for the different molecular traits, their possible mutational deterioration and the trade-offs between them is sound. We would expect the same qualitative (although not quantitative) results for the molecularly explicit, but unfeasible, type of simulation.

Even these oversimplified assumptions preserve the general properties of the macromolecule replicators that are most relevant to our problem. Although we can reliably calculate the two-dimensional structure of RNA molecules, this is not true for three-dimensional structures. Moreover, we do not know how to calculate the three pertinent replicator properties (replicase activity, replicase fidelity and template quality) from an arbitrary, given sequence. Thus we make the assumption that these are associated with separate parts of the molecule, and that they are in a three-way trade-off: in a macromolecule of a given length, one property can be enhanced at expense of the other two. Usually, RNA templates must bear a target structure in order to be accepted by contemporary RNA replicases made of protein[10]. Accuracy and speed are analysed in sufficient detail for DNA-dependent DNA polymerases. For example, there are mutator and antimutator mutants of the phage T4 polymerase, and the latter proceed more slowly on the DNA template[11,12]. In the polymerase of phage RB69, a close relative of phage T4, the polymerase active site and the exonuclease active site are 30 Å apart[13]. It seems that an important determinant of polymerase fidelity is geometric selection of Watson–Crick versus non-Watson–Crick base pairs[12], a result confirmed by recent visualization of DNA polymerase crystals[14,15]. It has been pointed out that the proposed mechanism could work for ribozyme replicases[16]. The three important replicase traits are expected to conflict with one another, especially in the stringent case of small molecules. But this is a conservative assumption, making the emergence of an efficient replicase population more difficult.

During a replication event mutations may occur, that is, the copy may differ from the template. For computational simplicity, base pairing is assumed to be homologous rather than complementary (that is, A pairs with A, C pairs with C, and so on). There are two types of mutation, as known for real replicases or polymerases.

The first type is addition and deletion mutations which occur at a

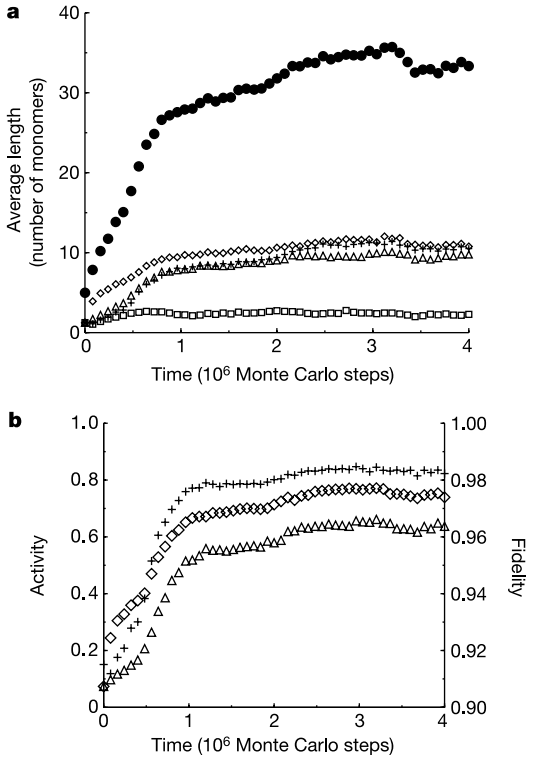

Figure 1 Long-term evolution of replicators (population-wide averages). **a**, Time series of length (closed circles) and of the amount of contributing A (open diamonds), B (open triangles), C (plus signs) and D monomers (open squares); **b**, Evolution of template (open diamonds), replicase (open triangles) catalytic activities and the fidelity of replication (pluses). Catalytic activities are scaled between 0 and 1, see equation (1). Parameter values: $\alpha_A = 0.1$; $\beta_A = 3$; $\gamma_A = 200$; $\alpha_B = 0.1$; $\beta_B = 3$; $\gamma_B = 200$; $\alpha_C = 0.9$; $\beta_C = 2$; $\gamma_C = 5$; $\mu = 6$; P_d (decay rate) = 0.001; $P_{ad} = 0.02$; no diffusion.

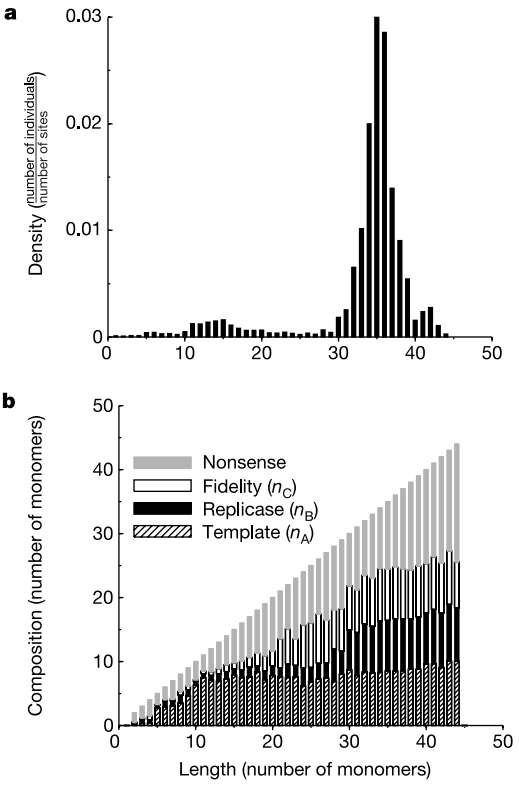

Figure 2 Distribution of replicators at the stationary state. **a**, Density of replicators of different length; **b**, Average length of template (hatched bars), replicase (black boxes), fidelity (white bars) functional sites and of nonsense parts (grey bars) within replicators of different lengths (nonsense parts include D monomers and shorter blocks of A, B and C monomers). (Parameters as before.)

constant probability $P_{ad} = 0.02$. Addition mutation attaches an extra monomer to the end of the molecule under copying; deletion mutation means that the copy breaks at a random position, and one of the fragments is lost, modelling damaging events. These mutations generate variance in the length of replicators.

The second type is that of point (substitution) mutations. Each monomer of the template chain is copied with accuracy equal to the replicase fidelity of the molecule acting as the replicase. If mutation occurs, then one of the three remaining monomer types is inserted into the copy, instead of the proper one.

At $t = 0$ half of the sites are 'inoculated' with five-monomer, random-sequence replicators, and we follow the evolution of the replicator population through many generations. Lineages producing sufficient numbers of accurate copies before decaying persist; others disappear from the selection arena. We show that selection favours the dominant quasispecies that possesses evolutionarily important properties. The quasispecies, thus developed, provides a good starting point for subsequent evolution under different selection pressures.

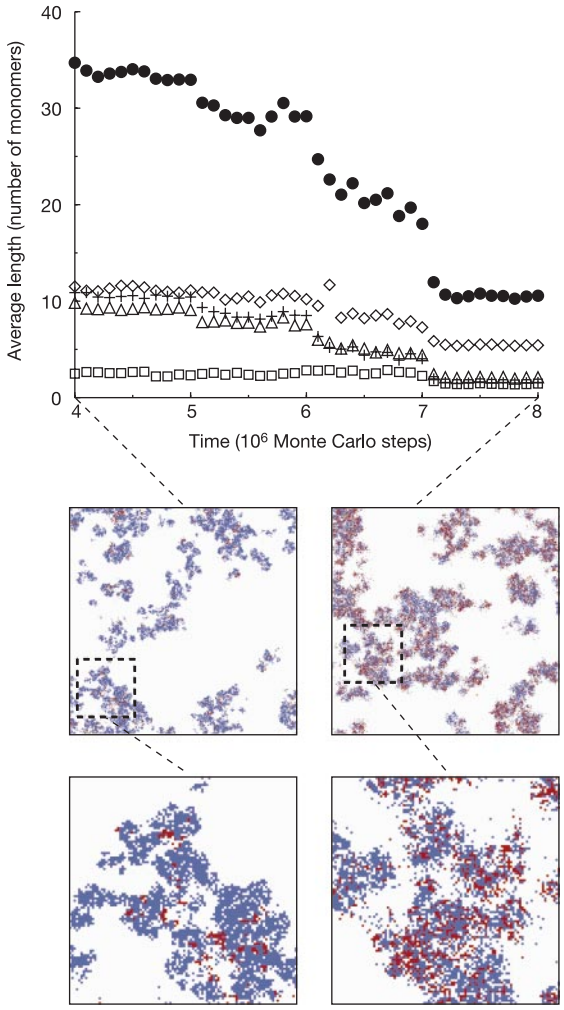

Figure 3 Replicator model with diffusion (population-wide averages). We start from the final state of Fig. 1 and increase diffusion rate step by step. Parameters as in Fig. 1, except diffusion rate: At $t = 4{,}000{,}000$ $D = 0.00001$ (replication event/movement due to a diffusion ratio of 12.5) and D jumps to 0.0001 (replication event/movement due to diffusion ratio of 1.6); 0.0002 and 0.0003 after every 10^6 Monte Carlo steps. Plates show the spatial distribution of replicators at $t = 4{,}000{,}000$ and $t = 8{,}000{,}000$ on two spatial scales. Upper plates show the whole arena; lower plates display an enlarged 100×100 part of it. Parasite and altruist replicators are distinguished on the basis of their lengths, according to Fig. 2a b. Parasites (replicators, shorter than 25) are represented in red; altruist replicators (at least 25 monomers) are represented in blue. Empty sites are white.

Starting from a population of oligomers with very limited functionality, complex, effective replicators emerge and spread (Fig. 1a, b). All the three important replicator properties (replicator activity and fidelity, and template quality) show considerable development. Selection favours replicators performing both replicase and template functions effectively and carrying out replication with high fidelity. The selective advantage of increasing template quality is obvious; a good template is replicated with higher probability by surrounding replicators. However, the selective advantage of replicase activity and of fidelity is a bit surprising. A replicator having these capabilities replicates its neighbours with higher probability, but it needs other efficient replicases around to spread. The advantage of these molecules comes from local interactions resulting in aggregated patterns, thus making reciprocal altruism between good replicases possible.

The monomers enhancing the replicase and template functions increase in number within the molecules, and they organize into functional sites. The evolutionary force shaping functional sites may be estimated by comparing the length of functional groups consisting of A, B and C monomers respectively, to the selectively neutral, contiguous D stretches, which are 5–10 times shorter than the length of the average functional site. The emergence of more complex functional sites results in an overall increase of the average length of replicators.

For selection in favour of faster and more accurate replicases to occur, even the least accurate replicases (those containing no C monomers) must have a fidelity significantly better than 0.25 (representing random monomer insertion), otherwise the system collapses in all cases, owing to the high error rate in replication. This is not a very strict restriction, given the inherent propensity for non-random monomer pairing in all known systems of template replication.

In the course of time this evolution comes to a halt. The diminishing (because of the sigmoid functions involved) advantage of extended functional sites is counterbalanced by the disadvantage of longer replication times due to increased template length. The population reaches a stable distribution of replicators of different lengths and functional structures (Fig. 2a, b). The maximum attainable length depends on the model parameters affecting replication, rather than on nutrient exhaustion. Although there are several sequences that differ in length and monomer sequence, we can distinguish two basic types. These two types show up as more or less distinct peaks in the sequence distribution (Fig. 2a). On one hand, large, complex replicators with strong replicase activity and high fidelity exist, which also serve well as templates. On the other hand, there is a smaller peak of short molecules with limited function as replicases, but with high template quality. These act as parasites of the dominant quasispecies: they could not exist without the replicase but themselves lacking replicase activity they do not contribute to the 'common good'.

Local interactions and limited dispersion guarantee that the parasites are not able to spread beyond a certain limit; therefore they cannot competitively exclude good replicators. To demonstrate the key role spatial structure plays in restraining parasites, we constructed the mean-field counterpart of the model, in which each template is copied by an 'average replicase': a molecule possessing the average of replicase activity and fidelity over the whole grid. In the mean-field model, starting from an initial population of replicators built up in previous runs, the density of individuals decreases abruptly, and ultimately the whole population goes extinct. The spatial model, incorporating diffusion[17], reveals the causes of this process. Increasing diffusion destroys the clustering of the altruists; replicator molecules gradually lose fidelity; all three replicator functions decline, template quality declines last, (Fig. 3). We recorded the ratio of 'birth' and movement events corresponding to particular diffusion rates. A slight diffusion does

not alter the results, and if the rate of birth and movement events is of the same order of magnitude, the results remain qualitatively the same. Impeding the evolution requires substantial mixing (see Fig. 3 legend). Our results agree with those from previous spatially explicit population dynamics of replicators, assuming either surface bonding[18,19] or protocellular compartmentation[20].

To show the robustness of the results we have done additional runs with different parameter values in the functions $t(n_A)$, $r(n_B)$. This difference between the functions is expressed by their half-saturation values (ν_h). The results did not show qualitative differences: in all cases the same evolutionary process takes place. At higher ν_h values longer sequences build up, because in this case the assemblage of effective catalytic sites requires more monomers.

We consider what would happen to the system using an analogous algorithm assuming complementary base pairing. Owing to the tradeoffs involved, it is quite conceivable that a strand complementary to an excellent replicase would be an excellent template. This may aid the spread of function and would point into the spontaneous emergence of complementary genic and enzymatic strands, and a primitive form of transcription (biased replication), in the spirit of the qualitative scenario of ref. 21.

The aim of our model is to show that certain molecular traits, crucial to the origin of life, can spread under plausible circumstances. We note that the selective scenario simulated here is compatible with existing theories and experiments. Examples of such approaches are the 'polymerization on the rocks'[22,23] (that is, chemical evolution on mineral surfaces likened to a primordial 'crêpes'[24]) and the surface-promoted amplification[25,26] chemical scenarios. Moreover, our simulation strengthens the view[18,19] that selection dynamics on mineral surfaces could have had an important positive effect on the dynamical coexistence of useful molecules of a primitive genetic system. How exactly, from a chemical point of view, this important phase of prebiotic evolution happened, is an open question. One possible scenario is based on ligation, leading from small templates and chemical ligation of long complementary building blocks, to long templates and enzymatic ligation of short substrates, culminating in template-directed polymerization by successive monomer addition[4]. The assumption used here that even very short oligonucleotides could act as rudimentary replicases is unrealistic[1]. A recently selected ribozyme is able to catalyse polymerization on an external template, up to the length of 14 nucleotides with an average accuracy of 0.967 per nucleotide[27]. There are three snags: the ribozyme itself is over 180 nucleotides long; its efficiency (speed) is not high enough; and template and copy are not separated. The basic message of the model remains valid if we shift the minimum replicase length to realistic values, but computation becomes more cumbersome. At present, the only hope is that an efficient non-enzymatic RNA replication system will be found[1,2] that could produce molecules long enough for a generalized replicase function. Once this is shown, further evolution is feasible by reciprocal molecular altruism 'on the rocks'. □

Methods

We have simulated the evolution of a large initial population of short replicators in a stochastic cellular automaton, because we suspect that spatial aspects play a decisive role in the dynamics of this system. The replication surface is a 400 × 400 square grid of toroidal topology to avoid edge effects. Each cell of the grid may be empty, or occupied by a replicator. An occupied cell is characterized by the sequence of the replicator it harbours. In each Monte Carlo step every site of the grid is updated exactly once, in a random order, according to the following rules:

(1) If the site is empty, nothing happens;

(2) If it is occupied, then with probability P_d the resident replicator decays;

(3) If the replicator survives, then it is a potential template and replicates (a new replicator is 'born') with probability $P_r = \frac{s}{3} dr \frac{t}{n}$ (where s is the number of potential replicators on the four neighbouring sites; r is replicase activity of one of the neighbouring replicators, chosen randomly; t is the template efficiency of the focal replicator; n is the number of monomers in the template.) d is a global variable that describes the density of available monomers for replicators. Its value is the same all over the grid, which is a reasonable assumption, if we assume that diffusion of monomers is fast. $d = \frac{\mu - m}{\mu}$, where $m = \sum_{1 \le i,j \le l} n_{i,j}/l^2$, summed over the grid ($\mu$ is a monomer abundance determining constant, $n_{i,j}$ is the length of replicator at position i,j and l is the length of sides of the square grid).

In the diffusive version a diffusion step occurs, by using the Toffoli–Margolus algorithm on a randomly chosen 2 × 2 square with probability D.

It would be tempting to identify our abstract monomers with real RNA bases. For example, in an experimental investigation of nonenzymatic template oligomerization[9]. It was found that cytidine acts like our monomer A. Yet our usage of the abstract monomers amounts to a subtle encoding as follows. Imagine that we assign a random (arbitrary) base sequence to a catalytic domain, such as AGGUGCCGAA. Then we encode this domain for our simulation as, say, BBBBBBBBBB. So abstract 'B' means any real base improving the activity in the given domain. A single base change may either destroy any function (which we handle by the dummy D), improve both (which is then no problem for evolution), or improve one function and diminish another.

The algorithm including diffusion is available at ftp://hera.colbud.hu/users/szathmary/replik.c

Received 8 May; accepted 13 September 2002; doi:10.1038/nature01187.

1. Joyce, G. F. & Orgel, L. E. in *The RNA World*, 2nd edn (eds Gesteland, R. F., Cech, T. R. & Atkins, J. F.) 49–77 (Cold Spring Harbor Laboratory Press, Cold Spring Harbor, New York, 1999).
2. Eigen, M. Self-organization of matter and the evolution of biological macromolecules. *Naturwissenschatten* **58,** 465–523 (1971).
3. Poole, A., Jeffares, D. & Penny, D. Early evolution: the new kids on the block. *BioEssays* **21,** 880–889 (1999).
4. James, K. D. & Ellington, A. D. The fidelity of template-directed oligonucleotide ligation and the inevitability of polymerase function. *Orig. Life Evol. Biosphere* **29,** 375–390 (1998).
5. Scheuring, I. Avoiding catch-22 of early evolution by stepwise increase in copying fidelity. *Selection* **1,** 135–145 (2000).
6. Wolfram, S. *A New Kind of Science* (Wolfram Media, Champaign, Illinois, 2002).
7. Trivers, R. L. The evolution of reciprocal altruism. *Q. Rev. Biol.* **46,** 35–57 (1971).
8. Nowak, M. & Sigmund, K. Tit for tat in heterogeneous populations. *Nature* **355,** 250–253 (1992).
9. Inoue, T. & Orgel, L. E. A nonenzymatic RNA polymerase model. *Science* **219,** 859–862 (1983).
10. Florentz, C. & Giegé, R. *tRNA: Structure, Biosynthesis, Function* (eds Söll, D. & RajBhandary, U. L.) 141–164 (American Society of Microbiology Press, Washington, 1995).
11. Galas, D. J. & Branscomb, E. W. Enzymatic determinants of DNA polymerase accuracy. Theory of coliphage T4 polymerase mechanisms. *J. Molec. Biol.* **124,** 653–687 (1978).
12. Goodman, M. F. & Fygenson, D. K. DNA polymerase fidelity: From genetics toward a biochemical understanding. *Genetics* **148,** 1475–1482 (1998).
13. Wang, J. *et al.* Crystal structure of a pol α family replication DNA polymerase from bacteriophage RB69. *Cell* **89,** 1087–1099 (1997).
14. Doublié, S. *et al.* Crystal structure of a bacteriophage T7 DNA replication complex at 2.2 Å resolution. *Nature* **391,** 251–258 (1998).
15. Kiefer, J. R. *et al.* Visualizing DNA replication in a catalytically active *Bacillus* DNA polymerase crystal. *Nature* **391,** 304–307 (1998).
16. Steitz, T. A. Structural biology. A mechanism for all polymerases. *Nature* **391,** 231–232 (1998).
17. Toffoli, T. & Margolus, N. *Cellular Automata Machines: A New Environment for Modeling* 155–167 (MIT Press, Cambridge, Massachusetts, 1987).
18. Boerlijst, M. C. & Hogeweg, P. Spiral wave structure in prebiotic evolution: Hypercycles stable against parasites. *Physica D.* **48,** 17–28 (1991).
19. Czárán, T. & Szathmáry, E. *The Geometry of Ecological Interactions: Simplifying Spatial Complexity* 116–134 (Cambridge Univ. Press, Cambridge, 2000).
20. Szathmáry, E. & Demeter, L. Group selection of early replicators and the origin of life. *J. Theoret. Biol.* **128,** 463–486 (1987).
21. Szathmáry, E. & Maynard Smith, J. The origin of chromosomes II. Molecular mechanisms. *J. Theoret. Biol.* **164,** 447–454 (1993).
22. Ferris, J. P. *et al.* Synthesis of long prebiotic oligomers on mineral surfaces. *Nature* **381,** 59–61 (1996).
23. Orgel, L. E. Polymerisation on the rocks: Theoretical introduction. *Orig. Life Evol. Biosphere* **28,** 227–234 (1998).
24. von Kiedrowski, G. Primordial soup or crêpes? *Nature* **381,** 20–21 (1996).
25. von Kiedrowski, G. Surface-promoted replication and exponential amplification of DNA analogues. *Nature* **396,** 245–248 (1998).
26. von Kiedrowski, G. & Szathmáry, E. Selection *versus* coexistence of parabolic replicators spreading on surfaces. *Selection* **1,** 173–179 (2000).
27. Johnston, W. K. *et al.* RNA-catalyzed RNA polymerization: accurate and general RNA-templated primer extension. *Science* **292,** 1319–1325 (2001).

Acknowledgements Financial support by the National Research Fund (OTKA) is gratefully acknowledged.

Competing interests statement The authors declare that they have no competing financial interests.

Correspondence and requests for materials should be addressed to E.S. (e-mail: szathmary@colbud.hu).